

# Electronic and magnetic properties of the $\text{Ti}_5\text{O}_9$ Magnéli phase

I. Slipukhina\* and M. Ležaić

Peter Grünberg Institut and Institute for Advanced Simulation,  
Forschungszentrum Jülich and JARA, D-52425 Jülich, Germany

(Dated: August 13, 2014)

Structural, electronic and magnetic properties of  $\text{Ti}_5\text{O}_9$  have been studied by *ab initio* methods in low-, intermediate- and high-temperature phases. We have found the charge and orbital order in all three phases to be non-stable, and the formation of  $\text{Ti}^{3+}$ - $\text{Ti}^{3+}$  bipolaronic states less likely as compared to  $\text{Ti}_4\text{O}_7$ . Several quasidegenerate magnetic configurations were calculated to have different width of the band gap, suggesting that the reordering of the unpaired spins at  $\text{Ti}^{3+}$  ions might at least partially be responsible for the changes in conductivity of this material.

PACS numbers: 31.15.A-, 71.20.-b, 75.25.Dk, 71.30.+h, 75.47.Lx

## I. INTRODUCTION

For several decades binary transition-metal oxides and related compounds have attracted increasing attention as resistive-switching materials. These are materials which can be switched between a high- and a low-resistance states and are very promising candidates for the next generation non-volatile resistive random access memory (RRAM). The resistive switching in many of these technologically relevant oxides is claimed to be based on the formation and disruption of highly-conductive filaments, through which the current flow is realized. However, still very little is known about the composition, structure and dimensions of these filaments.

Recent low-temperature conductivity and in situ current-voltage measurements confirmed that the conducting filaments in  $\text{Pt}/\text{TiO}_2/\text{Pt}^1$ , as well as Fe-doped  $\text{SrTiO}_3^2$  are composed of  $\text{Ti}_4\text{O}_7$  and  $\text{Ti}_5\text{O}_9$  Magnéli phases and their mixtures. These compounds belong to the homologous series  $\text{Ti}_n\text{O}_{2n-1}$  ( $3 \leq n \leq 9$ ) of Ti oxides with  $\text{TiO}_2$  and  $\text{Ti}_2\text{O}_3$  as the end members. Structurally they are related with rutile: there are adjacent rutile-like chains of  $n$  edge-sharing  $\text{TiO}_6$  octahedra, running parallel to the pseudorutile  $c_R$  axis (see Fig.1); the octahedra at the end of each of the chains share their faces with the next pseudorutile chain. With the exception of  $\text{Ti}_2\text{O}_3$ , these compounds possess a triclinic structure and they are mixed-valence compounds with two  $\text{Ti}^{3+}$  ( $3d^1$  electronic configuration) and  $(n-2)$   $\text{Ti}^{4+}$  ( $3d^0$ ) ions per formula unit (in an ionic picture). Several members of this homologous series, as well as the isostructural vanadium Magnéli phases  $\text{V}_n\text{O}_{2n-1}$ , are known to exhibit phase transitions with temperature, at which their conductivity changes drastically (it is the largest for  $n=3, 4$  and 5 and reduces for the members with higher  $n$ ). These transitions were interpreted in terms of the localization of the electrons in the cation sublattice. Indeed, the presence of both  $\text{Ti}^{3+}$  and  $\text{Ti}^{4+}$  ions provides several possibilities of charge distribution at cation sites, resulting in various charge-ordered states.

Take  $\text{Ti}_4\text{O}_7$  for example, which undergoes two consecutive phase transitions with temperature: a semiconductor-semiconductor transition at 130 K and

a semiconductor-metal transition at 150 K<sup>3</sup>. X-Ray diffraction studies<sup>4</sup> on  $\text{Ti}_4\text{O}_7$  single-crystals revealed that at low temperatures  $\text{Ti}^{3+}$  ions are covalently bonded to form the so-called *bipolarons* – singlet electron pairs ( $\text{Ti}^{3+}$ - $\text{Ti}^{3+}$  pairs). In the low-temperature (LT) semiconducting phase these pairs order so that they occupy alternate pseudorutile chains. In the high-temperature (HT) phase the pairing is believed to be absent and all the Ti-cations are in the same oxidation state  $\text{Ti}^{3.5+}$ , resulting in further increase of the conductivity and metallic behavior. The nature of the intermediate temperature (IT) phase remains rather unclear, however it is commonly believed that the (semiconductor-semiconductor) transition from LT to IT phase is accompanied with the reordering of the  $\text{Ti}^{3+}$ - $\text{Ti}^{3+}$  pairs<sup>4</sup>. It was assumed that in the IT phase bipolarons distribute in Ti-chains with a long-range order that requires a fivefold superstructure (bipolaron liquid state<sup>5</sup>). Later, the structure of the IT phase was revisited and suggested to be more complicated with the presence of bipolarons and a long-range order of Ti valences<sup>6</sup>. Recent photoemission experiments<sup>7</sup> interpreted the IT phase in  $\text{Ti}_4\text{O}_7$  as a highly anomalous state sandwiched between the mixed-valent Fermi liquid (HT phase) and charge ordered Mott-insulating phase (LT phase).

Two distinct phase transitions were also observed in  $\text{Ti}_5\text{O}_9$ , at 128 K and 139 K, accompanied by the conductivity decrease by a factor of 3 (Ref. 8) (or 50 according to Bartolomew and Frankl<sup>9</sup>). While LT and IT phases are found to be semiconducting, the conductivity in the HT phase increases with increasing temperature, which means that this phase is not a true metal and its nature is not clear. Compared to  $\text{Ti}_4\text{O}_7$ , for which a stable charge-ordered state was shown to exist at low temperature, the charge order in  $\text{Ti}_5\text{O}_9$  is rather uncertain, since the number of Ti ions in the pseudorutile chains is odd, preventing the formation of the  $\text{Ti}^{3+}$  long-range ordered pairs. X-ray studies performed by Marezio *et al*<sup>8</sup>, did not reveal any localization of charges and/or formation of covalent bonds between the  $\text{Ti}^{3+}$  cations in  $\text{Ti}_5\text{O}_9$ . However, in order to explain the semiconducting properties of the LT and IT phases, which in  $\text{Ti}_4\text{O}_7$  are related with the formation of  $\text{Ti}^{3+}$ - $\text{Ti}^{3+}$  pairs, they suggested a microdomain

structure of the material with  $\text{Ti}^{3+}$  mostly present at domain walls, making the detection of the charge localization and  $\text{Ti}^{3+}$ - $\text{Ti}^{3+}$  bonds formation by x-ray techniques rather impossible. The observed EPR signal the authors associated with the presence of unpaired  $\text{Ti}^{3+}$ . Watanabe<sup>10</sup> has recently studied the structural changes across the phase transitions in Magnéli phases by means of Raman spectroscopy. He observed two semiconductor-semiconductor transitions, at 137 K and 130 K, and revealed a fine structure of the LT phase, somewhat resembling the IT phase of  $\text{Ti}_4\text{O}_7$ . He suggested a considerable disorder for the LT phase of  $\text{Ti}_5\text{O}_9$  and a rather itinerant nature of the  $3d$  electrons in the IT and HT phases as in the HT phase of  $\text{Ti}_4\text{O}_7$ . The author did not observe any clear tendency as to the nature of the charge ordering in the considered Magnéli phases and concluded that in the compounds with odd  $n$  like  $\text{Ti}_5\text{O}_9$  the charge order is unstable.

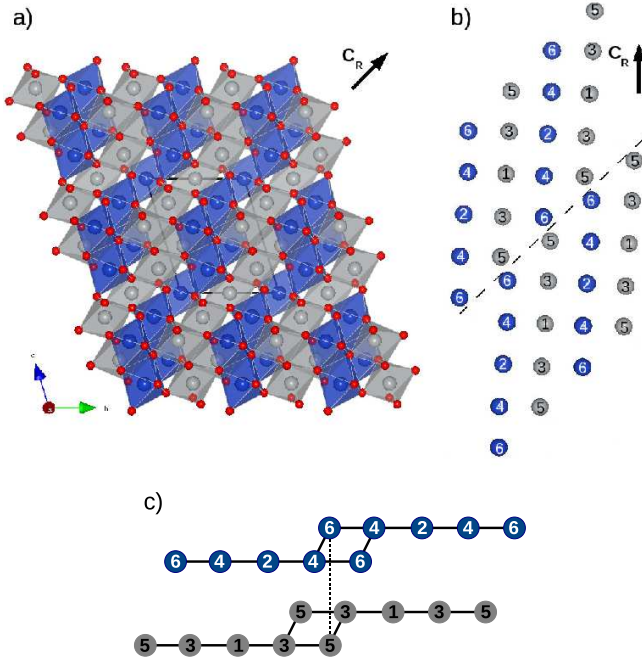


Figure 1: (color online) The crystal structure of the  $\text{Ti}_5\text{O}_9$ : spatial view (a), schematic view of the chain structure (b) and two adjacent Ti chains (c). The Ti atoms in the adjacent chains, which run parallel to the pseudorutile  $c_R$  axis, are shown in grey and blue, while oxygen atoms are shown in red. The black dashed line indicates the shear plane.

The effect of pressure on the phase transitions in  $\text{Ti}_n\text{O}_{2n-1}$  ( $n=4, 5, 6$ ) Magnéli phases was studied in Ref. 11. In contrast to a commonly accepted bipolaronic picture of the metal-insulator transition in these compounds, which is attributed to the strong electron-lattice coupling, the authors proposed their own explanations of the physics behind the phase transitions. The remarkably enhanced pressure effect on the phase transition temperatures as  $n$  goes from 6 to 4 the authors explained by

a delicate interplay between the electron-lattice coupling and electron correlations. In this respect charge ordering in  $\text{Ti}_4\text{O}_7$  is explained to be due to a dominant electron correlations with a subsequent bipolarons formation by an electron-lattice coupling.  $\text{Ti}_6\text{O}_{11}$ , on the contrary, is believed to be a small polaron insulator due to a prevailing electron-lattice coupling.  $\text{Ti}_5\text{O}_9$  is suggested to be in between these two extreme cases. The formation of small polarons, localized on one atomic site and randomly distributed over the lattice, explains rather well the unclear charge distribution in higher  $n$  Magnéli phases, observed in earlier experimental works<sup>8,12</sup>. The substantial Curie contribution, observed in  $\text{Ti}_5\text{O}_9$  at low temperatures<sup>13</sup>, which can be associated with the presence of upaired localized moments, is also in line with the proposed small polaron picture. A distinct pressure dependence of the resistivity in the HT phase of  $\text{Ti}_5\text{O}_9$  allowed the authors to assume that the system is just at the crossover region from large to small polarons. Such crossover in the systems with intermediate electron-coupling is often associated with a metal-insulator transition.

As for the magnetic properties,  $\text{Ti}_5\text{O}_9$ , as well as  $\text{Ti}_4\text{O}_7$  and  $\text{Ti}_6\text{O}_{11}$  phases show antiferromagnetic (AFM) behavior with Néel temperature ( $T_N$ ) of about 130 K<sup>14</sup>. According to magnetic susceptibility measurements in  $\text{Ti}_5\text{O}_9$ , there are two transitions which occur at 128 and 138 K, in contrast to  $\text{Ti}_4\text{O}_7$  with only one transition in magnetic susceptibility. The  $T_N$  is very close to the phase transition temperature, which allows one to relate the magnetic ordering with the phase transitions observed in this compound. At low temperatures ( $T < 40$  K) the measurements show a Curie behavior, while for the  $40 \text{ K} < T < 128 \text{ K}$  the temperature-independent susceptibility might be due to Van Vleck paramagnetism. Susceptibility in the HT phase is clearly temperature independent. Based on the measured molar susceptibility in Ti oxides, the effective magnetic moment for  $\text{Ti}_5\text{O}_9$  was calculated to be of  $0.245 \mu_B$  and it was concluded that a relatively small percentage of the unpaired electrons (7.4%) contributes to the Curie-Weiss behavior, while a large percentage (92.6%) contributes to its metallic (free electron gas) behavior; the small Weiss constant indicates that these spins do not interact strongly<sup>15</sup>.

Although rather well studied experimentally, there is very little known about the mechanism behind the transitions in Magnéli phases theoretically. Up to today, there are only a few DFT calculations on  $\text{Ti}_4\text{O}_7$ <sup>16–20</sup>, and to our knowledge, they are completely lacking for higher- $n$  phases. Therefore, in this work we aimed to develop a fundamental understanding of the mechanisms that underlie the phase transitions in Magnéli phases like  $\text{Ti}_5\text{O}_9$ , which, due to its high electrical conductivity and chemical stability, has a promising application not only in electrochemical engineering, but even in medicine as a neural stimulation electrode<sup>21</sup>. With this aim we performed DFT calculations in order to illuminate the changes in its electronic structure on a microscopic level and establish relations between the structural, electronic and magnetic

properties and their implications for conductive phenomena. We believe that the obtained results will be helpful in interpreting the physics of resistively switching Ti oxides.

## II. COMPUTATIONAL DETAILS

The electronic and magnetic properties of the different phases of  $\text{Ti}_5\text{O}_9$  were studied within the DFT, using the Vienna *ab initio* Simulation Package (VASP)<sup>22,23</sup> with projector augmented potentials (PAW)<sup>24,25</sup>. Kinetic energy cut-off of 450 eV and  $6 \times 6 \times 6$   $\mathbf{k}$ -points mesh was used for the unit cell of 28 atoms. The exchange correlation functional was treated within the generalized gradient approximation (GGA)<sup>26,27</sup>. GGA+ $U$  approximation in Dudarev's approach<sup>28</sup> with  $U$  applied to 3d states of Ti was used to take into account the electronic correlations.

The structural data for all three phases have been taken from the Ref. 8. The structure optimization was performed only for the LT phase with the aim to find the ground state of the system under study. For the sake of simplicity, we do not consider the spin-orbit coupling in our calculations, and we restrict ourselves to the collinear spins only.

## III. RESULTS AND DISCUSSION

### A. Correlation effects

It is known that oxygen deficient rutile  $\text{TiO}_{2-x}$  can be transformed into a Magnéli phase, when oxygen nonstoichiometry is sufficiently high ( $x > 0.001$ <sup>29</sup>). At such concentrations, oxygen vacancies arrange into extended defects, resulting in the shear plane structure (see Fig.1(c)). As a result, the defect states appear in the band gap close to the conduction band minimum, which are occupied by the electrons of  $\text{Ti}^{3+}$  ions. Numerous studies on  $\text{TiO}_{2-x}$ , including recent hybrid functional calculations<sup>30</sup>, have reported on the effect of the electronic correlations on the position of these defect states and the distribution of  $\text{Ti}^{3+}$  ions. For  $\text{Ti}_4\text{O}_7$  or  $\text{Ti}_5\text{O}_9$  with similar peculiarities of the electronic structure, + $U$  approach or hybrid functionals were used to correctly account for the correlation effects and were able to reproduce the ground state properties of the phases<sup>16-20</sup>. However, the correlations might be less effective in the phases with larger  $n$  (i.e., with smaller density of 3d electrons), as it was assumed in Ref. 10 based on the observed lack of the systematic trend in charge ordering in different Magnéli phases.

In order to elucidate the importance of electron correlations for the charge localization in  $\text{Ti}_5\text{O}_9$ , we have performed calculations within GGA+ $U$  approach, assuming the unit-cell model for the order/disorder of the  $\text{Ti}^{3+}$  and  $\text{Ti}^{4+}$  ions. To cover the limits of weak and strong electron interactions, the on-site Coulomb energy parameter was varied within the range  $0 < U < 6$  eV. The evolution

of the density of electronic states (DOS) with  $U$  in the LT phase with the experimental structure is presented in Fig.2; these calculations were performed assuming an AFM spin coupling with a zero total magnetic moment per cell.

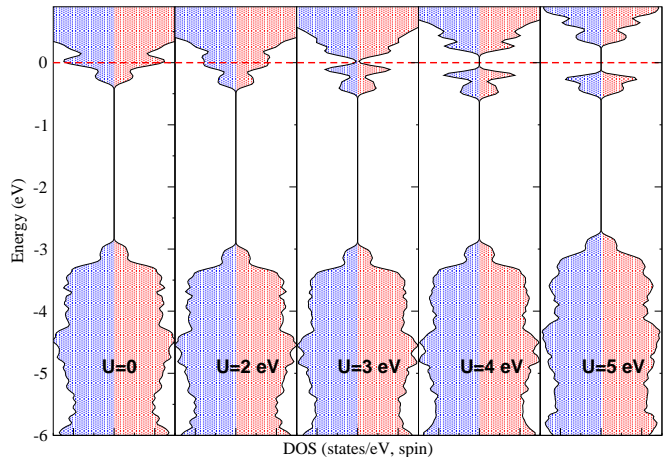


Figure 2: (color online) The GGA+ $U$  spin-polarized DOS, calculated for the LT phase of  $\text{Ti}_5\text{O}_9$  at different  $U$  for the AFM spin alignment. The Fermi level is at zero energy (shown by red dashed line). Blue and red shading denotes the majority and minority spins, correspondingly.

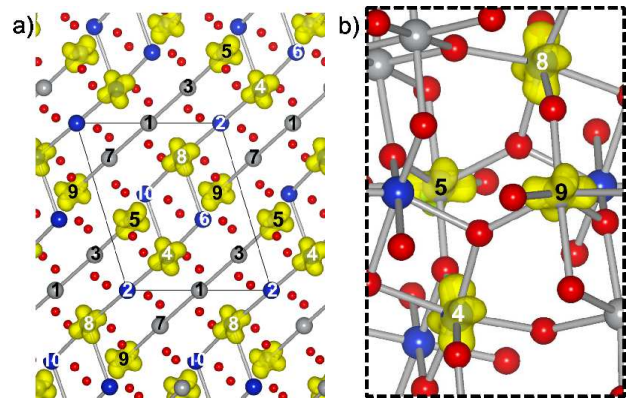


Figure 3: (color online) 3d valence charge distribution in the LT phase of  $\text{Ti}_5\text{O}_9$ : (a) general view with Ti-Ti bonds; (b) zoomed view with Ti-O bonds. The calculated charge density isosurfaces correspond to the  $\text{Ti}^{3+}$  gap states. The presented results were obtained at  $U = 6$  eV for the AFM spin configuration with  $M_{\text{tot}} = 0$ . Blue and grey colors distinguish between the Ti atoms in the adjacent pseudorutile chains. Note different orientation of the  $t_{2g}$ -like orbitals.

As follows from Fig.2, for  $U \leq 3$  eV the DOS remains metallic with Ti 3d states merged into the conduction band. A small band gap of about 0.1 eV between the occupied and unoccupied 3d states of Ti opens in both spin channels at  $U > 3$  eV, and it increases up to 0.7 eV at  $U = 6$  eV (see Tab.I). It should be noted that an



Table I: The GGA+ $U$  absolute values of magnetic moments  $|M|$  (in  $\mu_B$ ) at Ti sites in the LT phase of  $\text{Ti}_5\text{O}_9$ , calculated for different  $U$  (at  $J = 1$  eV) for the AFM/FM spin alignment. The energy gaps  $E_g$  (in eV) and the total energy differences  $\Delta E = E_{AFM} - E_{FM}$  (in meV/f.u.) are also listed.

	$U=2$ eV	$U=3$ eV	$U=4$ eV	$U=5$ eV	$U=6$ eV
Ti(1)	0/0.21	0/0.23	0/0.15	0/0.14	0/0
Ti(2)	0/0.47	0/0.52	0/0.50	0/0.55	0/0.44
Ti(3)	0.29/0.30	0.37/0.43	0.38/0.45	0.28/0.44	0/0.56
Ti(4)	0.19/0.30	0.43/0.36	0.58/0.43	0.71/0.37	0.81/0.43
Ti(5)	0.27/0.19	0.32/0.47	0.37/0.49	0.53/0.61	0.77/0.59
Ti(6)	0/0.09	0/0.26	0/0.22	0/0.17	0/0.12
$E_g$	0/0	0/0	0.1/0	0.4/0	0.7/0
$\Delta E$	55	47	23	-19	-72

energy gap of 0.7 eV was also obtained for  $\text{Ti}_4\text{O}_7$  at  $U = 0.4$  Ry (5.4 eV) in Ref.19 (the choice of this value of  $U$  was justified by comparing the total energy difference between the three phases at different  $U$  with the transition temperatures). The topology of the insulating DOS very much resembles that of the  $\text{Ti}_4\text{O}_7$ <sup>17-19</sup>. The well-localized states just below the Fermi level are formed by the 3d orbitals of Ti possessing non-zero magnetic moment. Figure 3 shows the spatial distribution of these localized gap states, calculated at  $U = 6$  eV. It is clear that the system is not only charge ordered, but also orbitally-ordered: occupied orbitals at different  $\text{Ti}^{3+}$  sites are of  $d_{xy}$  and  $d_{xz}$  (or  $d_{yz}$ ) symmetry, if we define them in the local frame of the octahedra. While the conduction band is mainly contributed by Ti 3d states, the valence band originates from the oxygen 2p states (with a small admixture of Ti 3d states due to Ti-O bonds formation) and it is separated from the gap states by an energy interval, which is much larger than the fundamental gap. This gap decreases with the increasing  $U$  from around 2.8 eV at  $U = 0$  to 1.9 eV at  $U = 6$  eV. The width of the split-off 3d-band is decreasing as the electron localization increases with the increased  $U$ . Following the evolution of the DOS as a function of  $U$  parameter, it is difficult to make certain conclusions on the appropriate value of  $U$  in the case of  $\text{Ti}_5\text{O}_9$ , since the existing experimental data about the electronic band structure of Ti Magnéli phases is quite diverse. According to Mulay *et al*<sup>13</sup>, who studied the cooperative magnetic transitions in titanium oxides, the band gap of  $\text{Ti}_5\text{O}_9$  in the LT phase is found to be of 0.035 eV. The authors also report on the gap of 0.041 eV for  $\text{Ti}_4\text{O}_7$ , while optical measurements in Ref. 31 gave a band gap of 0.25 eV; later photoemission spectroscopy experiments revealed a gap of only 0.1 eV<sup>7</sup>. One is clear: even if the electron-electron interactions are less pronounced in  $\text{Ti}_5\text{O}_9$  than in the other Magnéli phases with higher concentration of 3d electrons, they play an important role in the stabilization of its insulating ground state.

Table II: Ti-O interatomic distances (in Å) in the LT (115 K) and HT( 295 K) phases of  $\text{Ti}_5\text{O}_9$  according to structural parameters from Ref.8

	115 K	295 K		115 K	295 K
Ti(1)-O(2)	1.949	1.955	Ti(4)-O(5)	1.978	1.987
Ti(1)-O(3)	1.963	1.970	Ti(4)-O(6)	2.085	2.095
Ti(1)-O(4)	2.009	2.015	Ti(4)-O(9)	2.086	2.092
Ti(2)-O(1)	2.013	2.008	Ti(5)-O(5)	1.849	1.842
Ti(2)-O(2)	1.973	1.974	Ti(5)-O(6)	2.055	2.053
Ti(2)-O(5)	2.004	2.007	Ti(5)-O(7)	2.145	2.155
Ti(3)-O(1)	1.903	1.906	Ti(5)-O(7)	2.002	1.992
Ti(3)-O(2)	1.939	1.929	Ti(5)-O(8)	1.956	1.943
Ti(3)-O(3)	1.991	1.976	Ti(5)-O(9)	2.045	2.040
Ti(3)-O(6)	2.029	2.035	Ti(6)-O(4)	1.879	1.883
Ti(3)-O(7)	2.075	2.071	Ti(6)-O(6)	2.143	2.133
Ti(3)-O(8)	2.081	2.086	Ti(6)-O(7)	1.991	2.003
Ti(4)-O(1)	1.942	1.943	Ti(6)-O(8)	1.855	1.856
Ti(4)-O(3)	1.902	1.907	Ti(6)-O(9)	2.196	2.186
Ti(4)-O(4)	2.007	1.995	Ti(6)-O(9)	1.976	1.981

Table III: Ti-Ti interatomic distances (in Å) in the LT (115 K), IT (135 K) and HT( 295 K) phases of  $\text{Ti}_5\text{O}_9$  according to structural parameters from Ref. 8

	115 K	135 K	295 K
Ti(1)-Ti(3)	2.930	2.932	2.928
Ti(2)-Ti(4)	2.906	2.908	2.924
Ti(3)-Ti(5)	2.979	2.989	3.004
Ti(4)-Ti(6)	3.037	3.043	3.041
Ti(5)-Ti(6)	2.827	2.816	2.829

## B. Structural effects

As mentioned earlier,  $\text{Ti}_5\text{O}_9$  crystallizes in the triclinic  $P\bar{1}$  structure with two formula units per unit cell. There are six crystallographically independent Ti atoms in its unit cell, surrounded by distorted oxygen octahedra (see Fig.1 and Tab.II). Among them Ti(1) and Ti(2) are at the center of symmetry, while the other eight atoms are related by inversion symmetry, namely  $\text{Ti}(3) \equiv \text{Ti}(7)$ ,  $\text{Ti}(4) \equiv \text{Ti}(8)$ ,  $\text{Ti}(5) \equiv \text{Ti}(9)$  and  $\text{Ti}(6) \equiv \text{Ti}(10)$ . These atoms form two crystallographically independent pseudorutile chains:  $\text{Ti}(5)-\text{Ti}(3)-\text{Ti}(1)-\text{Ti}(3)-\text{Ti}(5)$  and  $\text{Ti}(6)-\text{Ti}(4)-\text{Ti}(2)-\text{Ti}(4)-\text{Ti}(6)$ <sup>32</sup>. The Ti(5) and Ti(6) atoms are the nearest to the shear planes and their environment is not rutile-, but sesquioxide-like, similarly to the  $\text{Ti}_4\text{O}_7$ . The Ti(5)-Ti(6) distance is  $\sim 2.83$  Å and is the shortest in the lattice (see Table III). The Oxygen octahedra around these atoms are severely distorted (the difference in Ti-O distances is  $\sim 0.3$  Å) (see Table II). According to Ref. 8, the  $\text{Ti}(5)-\text{Ti}(3)-\text{Ti}(1)-\text{Ti}(3)-\text{Ti}(5)$  chains are more distorted than the  $\text{Ti}(6)-\text{Ti}(4)-\text{Ti}(2)-\text{Ti}(4)-\text{Ti}(6)$  one, and thus have a slightly larger separation of charge. However, as can be seen from Tab.III, these distortions are very small and structurally the low-temperature phases are almost identical to the HT phase. This is not the case

for  $\text{Ti}_4\text{O}_7$ , where the formation of bipolarons in the LT phase and their rearrangement into polarons and bipolarons in the IT phase with the consequent collapse in the HT phase are clearly related with the electron-lattice coupling. The transition from HT to LT phase in  $\text{Ti}_4\text{O}_7$  is accompanied by an essential decrease in the Ti-Ti distances ( $\sim 0.2$  Å) with a consequent charge localization at Ti ions, involved in longer Ti-O and shorter Ti-Ti bonds. Interestingly, in the isostructural  $\text{V}_4\text{O}_7$  no changes in cation-cation distances larger than  $\sim 0.06$  Å are observed at the phase transition, despite the clear separation of charge into  $\text{V}^{3+}$  and  $\text{V}^{4+}$  in the alternate chains. Similar behavior applies to another member of the vanadium series,  $\text{V}_5\text{O}_9$ , which undergoes a metal-insulator transition at 135 K<sup>32</sup>. Although incomplete, V-V dimerization is clearly observed in  $\text{V}_4\text{O}_7$ <sup>33</sup>, while it is negligible in  $\text{V}_5\text{O}_9$ <sup>34</sup>. It was speculated that there are many different bonding patterns in the latter two compounds, and that an average of these patterns is observed by the classical x-ray diffraction methods<sup>32</sup>.

Obviously, if the insulating behavior was induced by the lattice distortions only, the crystalline symmetry below the phase transition would be lower than in the metallic region. However, this is not the case in the  $\text{Ti}_5\text{O}_9$  crystal, although its LT phase is slightly more distorted than the HT one. To find out how these small lattice distortions at the phase transitions affect the electronic properties of  $\text{Ti}_5\text{O}_9$ , we performed total-energy calculations for the experimental structures<sup>8</sup> of all three phases. Figure 4 shows the density of states (DOS) of  $\text{Ti}_5\text{O}_9$ , calculated at  $U=5$  eV for the LT, IT and HT structures (as reported by Marezio *et al*<sup>8</sup>), assuming an AFM spin ordering with zero total moment per cell. One can clearly see that the DOS for all the three phases is very similar to each other. They all are insulating with the band gap in the LT phase of about 0.43 eV and only slightly smaller gap of 0.38 eV in the IT and HT phases. The corresponding charge distribution is similar from phase to phase with only a slight difference in the Ti magnetic moments (see Tables IV and V for  $M_{\text{tot}} = 0$ ). Therefore, although the peculiarities of the crystalline structure of  $\text{Ti}_5\text{O}_9$  are certainly reflected in the rich variety of the possible charge order patterns, the lattice distortions at the phase transitions are rather insignificant to have a crucial effect on the conducting properties of the material.

### C. Magnetic and charge order

To find the ground state magnetic ordering and which Ti atoms participate in it, we have considered an antiferromagnetic and a ferromagnetic (FM) spin configuration along with a non-magnetic one (which turned out to be much higher in energy for all three phases). First, we have considered the effect of electron correlations on the magnetic behavior of the crystal. For the experimental structures we have found that at  $U \leq 4$  eV the LT phase

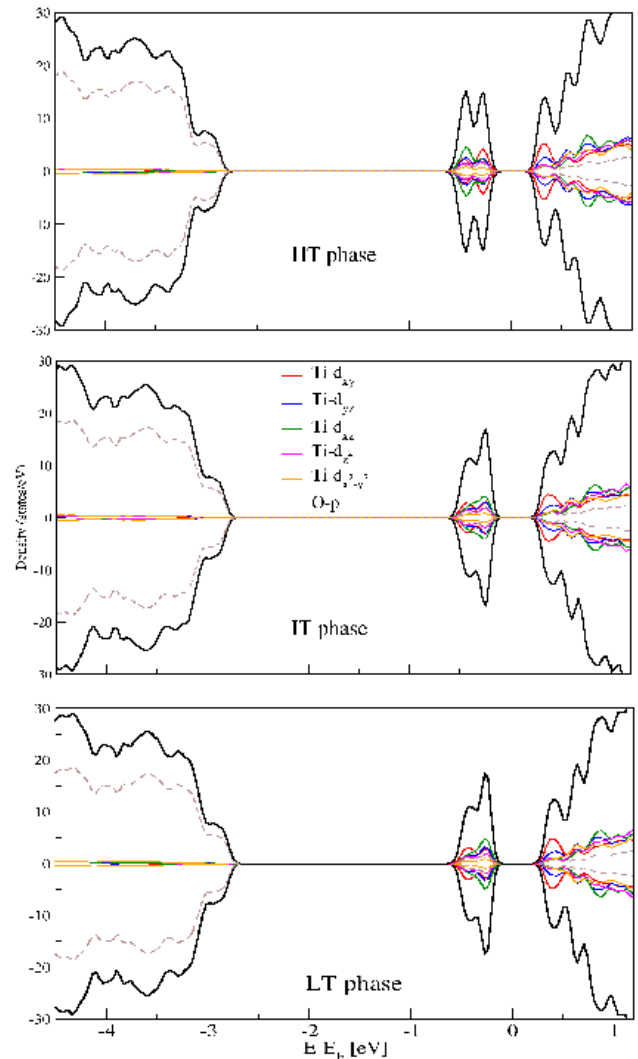


Figure 4: (color online) The GGA+ $U$  spin-polarized density of electronic states (DOS), calculated for the LT, IT and HT phases of  $\text{Ti}_5\text{O}_9$  at  $U = 5$  for the AFM spin alignment (the lowest-energy configuration on Fig.5). Positive (negative) values indicate spin-up (spin-down) DOS.

is FM and metallic, while for larger  $U$  it tends to be an AFM insulator (see Table I). Depending on the chosen  $U$  and the resulting spin configuration, the calculated magnetic moments on each of the inequivalent Ti atoms vary within the range 0.1-0.8  $\mu_B$ . This is in contrast to  $\text{Ti}_4\text{O}_7$ , for which the ionic magnetic moments in the LT phase were calculated to be robust with respect to their relative orientation and thus were linked to the local structure around Ti<sup>19</sup>. As follows from Table I, even in the FM state the magnetic moment is distributed among all the Ti atoms somewhat inhomogeneously. In the AFM state the charge disproportionation is more pronounced within the whole range of  $U$  values and non-zero moment is observed only at Ti(3), Ti(4) and Ti(5) sites. While Ti(4)

and Ti(5) magnetic moments increase with increasing  $U$ , the moment at Ti(3) site starts to decrease for  $U > 4$  and is completely suppressed at  $U = 6$  eV (nominal  $\text{Ti}^{3+}$  and  $\text{Ti}^{4+}$  ions become clearly distinguishable). When Ti(3) moment becomes zero, the charge order pattern is symmetric with respect to the inversion. At the FM spin alignment the behavior is somewhat different: the charge order pattern is less symmetric, but more homogeneous, and it is less sensitive to the changes of  $U$  value. As a result, the energy gap is zero for the whole range of  $U$  values.

We have performed fixed spin moment calculations for all three phases by calculating the total energy at the constrained magnetic moment of the unit cell. The results, obtained for  $U = 5$  eV, are presented in Tab.IV and Tab.V. It is clear from the listed data that there are several stable magnetic configurations with a very small relative energy difference, namely the configurations with total moment of 0 (AFM), 2 and  $4 \mu_B/\text{cell}$ . Moreover, for each of the magnetic configurations we have obtained a whole set of different possible charge order patterns (see Fig.5); therefore, we present here only those which in our calculations have the lowest energy.

### 1. Low-temperature phase

For the experimental structure of the LT phase the configuration with the total magnetic moment  $M_{\text{tot}} = 2 \mu_B/\text{cell}$  is practically degenerate with the AFM configuration with  $M_{\text{tot}} = 0$  (the energy difference is only 6 meV/f.u.) (see Table IV). The FM configuration with  $M_{\text{tot}} = 4 \mu_B/\text{cell}$  is 20 meV/f.u. higher in energy than the AFM one. We observe stronger localization of the charge, and hence, larger band gap, for the configurations where more Ti moments are aligned antiparallel to each other: the band gap is the largest for the AFM state and it decreases to zero for the FM one. Therefore, opening of the gap in  $\text{Ti}_5\text{O}_9$  when going from high to low temperatures might be closely related with the AFM ordering of the unpaired spins. This is in line with the fact that experimentally the Néel temperature and the semiconductor-metal transition temperatures in this material nearly coincide.

Interestingly, as follows from Table IV, when structural relaxations are taken into account, the lowest energy charge distribution is the same for all the three magnetic configurations. It is such that  $\text{Ti}^{3+}$  ions (polarons) are at the position of Ti(4) and Ti(5) cations. Within a pseudorutile chain they are well separated by either one or three  $\text{Ti}^{4+}$  ions (Fig.3), retaining the inversion symmetry. While  $\text{Ti}^{3+}$  in the Ti(5) position has a common face with the  $\text{Ti}^{4+}$  at Ti(6) site across the shear plane, the  $\text{Ti}^{3+}$  in the Ti(4) position is close to the middle of the pseudorutile chain. It is clear from Fig. 3(b) that there is no direct overlap between the  $t_{2g}$  orbitals at Ti(4) and Ti(5) sites and the interaction between the corresponding electrons is realized through the hopping via bridging

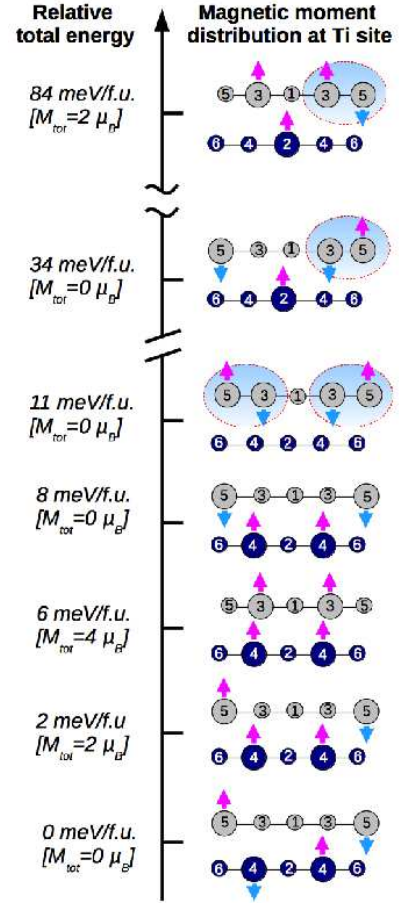


Figure 5: (color online) A schematic diagram showing the relative stability of several lowest-energy charge and magnetically ordered states, obtained for the LT phase taking into account structural relaxations. Shaded area within a red-dashed oval depicts  $\text{Ti}^{3+}$ - $\text{Ti}^{3+}$  singlet pairs (bipolarons). Dark blue and grey colors are used to distinguish between Ti in adjacent pseudorutile chains. Big (small) balls denote  $\text{Ti}^{3+}$  ( $\text{Ti}^{4+}$ ) ions.

oxygen.

Several decades ago, James and Catlow<sup>35</sup> theoretically predicted that the electrons created by the reduction of rutile or higher Magnéli phases should be trapped by the shear plane. In  $\text{Ti}_5\text{O}_9$  this would result in charge-order state with  $\text{Ti}^{3+}$  ions occupying Ti(5) and Ti(6) sites. However, in our calculations such state is  $\sim 148$  meV/f.u. less stable than the lowest-energy one with  $\text{Ti}^{3+}$  at Ti(5) and Ti(4) sites. This means that not all electrons occupy the sites adjacent to the shear planes, but prefer the localization at the nearest neighbor sites.

In contrast to the experimental structures, the localization of the charges in the relaxed structures is much stronger and it results in the insulating behavior even for the FM spin alignment. The total energy difference between the states with  $M_{\text{tot}} = 0, 2$  and  $4 \mu_B/\text{cell}$  is less than 10 meV/f.u. The fact that it is so small indicates that the charge and spin order is unstable. A large

Table IV: Magnetic moments on Ti atoms (in  $\mu_B$ ), total energies  $\Delta E$  with respect to the lowest-energy magnetic configuration (in meV/f.u.) and the band gap  $E_g$  (in eV), calculated for the experimental and relaxed (theoretical) structures of LT phase.

$M_{\text{tot}}$	$0 \mu_B/\text{cell}$		$2 \mu_B/\text{cell}$		$4 \mu_B/\text{cell}$	
$\mu_{\text{Ti}}$	exp.	relaxed	exp.	relaxed	exp.	relaxed
Ti(1)	0	0	0	0	0.14	0
Ti(2)	0	0	0.31	0	0.54	0
Ti(3)	-0.28	0	-0.17	0	0.44	0
Ti(4)	0.71	0.83	0.68	0.84	0.37	0.85
Ti(5)	-0.53	-0.81	-0.56	-0.80	0.61	0.84
Ti(6)	0	0	0	0	0.17	0
Ti(7)	0.28	0	0.32	0	0.44	0
Ti(8)	-0.71	-0.83	0.67	0.84	0.37	0.85
Ti(9)	0.53	0.81	0.55	0.83	0.61	0.84
Ti(10)	0	0	0	0	0.17	0
$\Delta E$	6	0	0	2	26	7
$E_g$	0.46	0.9	0.19	0.82	0	0.67

separation between the  $\text{Ti}^{3+}$  ions results in rather weak magnetic interactions, which is reflected in the small energy difference between the states with the same charge distribution, but different number of parallel/antiparallel spins. This is in line with the conclusions made by Dancy and Muley<sup>15</sup>, who observed small Weiss constant and hence weak interaction between the unpaired spins in  $\text{Ti}_5\text{O}_9$ . This is different from  $\text{Ti}_4\text{O}_7$ , for which the AFM interaction between the spins within the  $\text{Ti}^{3+}$ - $\text{Ti}^{3+}$  pairs was found to be rather strong<sup>17</sup>, although the inter-pair coupling was calculated to be much weaker. We have also considered the states, where four unpaired spins at Ti sites are distributed in the way to form bipolarons within the same pseudorutile chain, as well as the state with coexisting bipolarons and polarons. These states were obtained to be 11 meV/f.u. and 34 meV/f.u., correspondingly, higher in energy than the ground state and are both insulating. Therefore, the ground state of the LT phase of  $\text{Ti}_5\text{O}_9$  is semiconducting, however its charge order pattern is not unique.

## 2. Intermediate- and high-temperature phases

Since our *ab initio* calculations are performed at  $T = 0$  K temperature, for the IT and HT phases we have considered only the experimental structures as reported by Marezio *et al.*<sup>8</sup>. In analogy to the LT phase, we observe several stable magnetic configurations for the IT and HT phases, which are almost degenerate within our calculation error: these are the configurations with the total magnetic moment of 0, 2 and  $4 \mu_B/\text{cell}$ . For each of these magnetic configurations our fixed-spin moment calculations revealed several possible charge order patterns, but in Table V we present only the lowest-energy ones. For the IT phase the calculated band gap is the largest for the configuration with  $M_{\text{tot}} = 0 \mu_B/\text{cell}$  (about 0.4 eV)

Table V: Magnetic moments on Ti atoms (in  $\mu_B$ ),  $\Delta E$  total energies with respect to the lowest-energy magnetic configuration (in meV/f.u.) and the band gap  $E_g$  (in eV), calculated for the experimental structures of the IT and HT phases.

$M_{\text{tot}}$	$0 \mu_B/\text{cell}$		$2 \mu_B/\text{cell}$		$4 \mu_B/\text{cell}$	
$\mu_{\text{Ti}}$	IT	HT	IT	HT	IT	HT
Ti(1)	0	0	0	0	0.20	0
Ti(2)	0	0	0.35	0.27	0.68	0.29
Ti(3)	-0.25	-0.33	-0.13	-0.14	0.43	0.41
Ti(4)	0.71	0.73	0.67	0.70	0.19	0.70
Ti(5)	-0.55	-0.46	-0.58	-0.56	0.69	0.47
Ti(6)	0	0	0	0	0.19	0.14
Ti(7)	0.25	0.33	0.29	0.46	0.42	0.40
Ti(8)	-0.71	-0.73	0.64	0.69	0.19	0.70
Ti(9)	0.55	0.46	0.57	0.39	0.69	0.47
Ti(10)	0	0	0	0	0.19	0.14
$\Delta E$	9	8	0	2	2	0
$E_g$	0.43	0.38	0.15	0.25	0	0.04

and it is almost the same as the gap calculated for the experimental structure of the LT phase. The gap is somewhat smaller for the configuration with  $M_{\text{tot}} = 2 \mu_B/\text{cell}$  and completely vanishes when the spins are aligned ferromagnetically due to more homogeneous distribution of the valence charge. Similar tendency is also observed for the HT phase with the only difference being that the gap (although very small) is non-zero for the FM configuration. It should be noted that for the HT phase there is another FM state, which is metallic and has a more homogeneous charge distribution, but this state is about 30 meV/f.u. higher in energy.

The magnetic moments do not vary much from phase to phase, which once again indicates a secondary role of the crystal structure in the electronic properties of the  $\text{Ti}_5\text{O}_9$ . The charge distribution for the considered configurations resembles the one observed in the LT phase, however, it is slightly more localized for the FM configuration in the HT phase than in the LT or IT phases. However, the magnetic moment distribution remains inhomogeneous even for the FM configuration in the HT phase and does not correspond to the suggested  $\text{Ti}^{3.5}$  picture. Therefore, the local environment and distortions play a visible role in the magnetic moment distribution in this material.

## IV. CONCLUSIONS

In summary, we have performed first-principles calculations to study the electronic and magnetic properties of the  $\text{Ti}_5\text{O}_9$  crystal, which belongs to the homologous series of  $\text{Ti}_n\text{O}_{2n-1}$  oxides, known as Magnéli phases. From our results it is difficult to conclude on which charge distribution is realized in this material at different temperatures, since for all three phases we find several quasidegenerate magnetic solutions. We therefore assume that the charge order within the cation sublattice in  $\text{Ti}_5\text{O}_9$  is not unique



and thus unstable, which makes its experimental detection at finite temperatures difficult. We suggest that in contrast to  $\text{Ti}_4\text{O}_7$ , the formation of  $\text{Ti}^{3+}$ - $\text{Ti}^{3+}$  pairs in this compound is less likely, although not completely impossible, since a bipolaronic state is only slightly higher in energy than the ground state. Our calculations performed for all three phases showed that crystal structure changes at the transitions make a minor influence on the electronic structure of the compounds. Although the electronic correlations are important for the stabilization of the insulating ground state, the phase transitions in this compound are related to a greater extent to a reordering of the unpaired spins. This conclusion agrees well

with the antiferromagnetism model presented by Adler in Ref.36, where the author considered different scenarios for the metal-nonmetal transitions in transition metal oxides and sulfides. Thus, the mechanism behind the phase transitions in  $\text{Ti}_5\text{O}_9$  must be a complex interrelation between the electronic correlations, electron-lattice, as well spin-lattice coupling.

We appreciate the support of the Jülich Supercomputing Centre (Project JIFF38) and gratefully acknowledge the support of the SFB917-Nanoswitches and Young Investigators Group Program of the Helmholtz Association, Contract VH-NG-409.

- 
- \* Corresponding author: i.slipukhina@fz-juelich.de
- <sup>1</sup> D.-H. Kwon, K.M. Kim, J.H. Jang, J.M. Jeon, M.H. Lee, G.H. Kim, X.-S. Li, G.-S. Park, B. Lee, S. Han, M. Kim and C.S. Hwang, *Nature nanotechnology* **5**, 148 (2010).
  - <sup>2</sup> R. Münstermann, T. Menke, R. Dittmann and R. Waser, *Advanced Materials* **22**, 4819 (2010).
  - <sup>3</sup> M. Marezio, D.B. McWhan, P.D. Dernier and J.P. Remeika, *Phys. Rev. Lett.* **28**, 1391 (1972).
  - <sup>4</sup> M. Marezio, D.B. McWhan, P.D. Dernier and J.P. Remeika, *J. Solid State Chem* **6**, 213 (1973).
  - <sup>5</sup> S. Lakkis, C. Schlenker, B.K. Chakraverty, R. Buder and M. Marezio, *Phys. Rev. B* **14**, 1429 (1976).
  - <sup>6</sup> Y. Le Page and M. Marezio, *J. Solid State Chem.* **53**, 13 (1984).
  - <sup>7</sup> M. Taguchi, A. Chainani, R. Eguchi, Y. Takata, M. Yabashi, K. Tamasaku, Y. Nishino, T. Ishikawa, S. Tsuda, S. Watanabe, C.-T. Chen, Y. Senba, H. Ohashi, K. Fujiwara, Y. Nakamura, H. Takagi and S. Shin, *Phys. Rev. Lett.* **104**, 106401 (2010).
  - <sup>8</sup> M. Marezio, D. Tranqui, S. Lakkis and C. Schlenker, *Phys. Rev. B* **16**, 2811 (1977).
  - <sup>9</sup> R.F. Bartolomew and D.R. Frankl, *Phys. Rev.* **187**, 828 (1969).
  - <sup>10</sup> Masayuki Watanabe, *phys. stat. sol. (c)* **6**, 260 (2009).
  - <sup>11</sup> H. Ueda, K. Kitazawa, H. Takagi and T. Matsumoto, *J. Phys. Soc. Jap.* **71**, 1506 (2002).
  - <sup>12</sup> Y. Le Page and P. Strobel, *J. Solid State Chem.* **47**, 6 (1983).
  - <sup>13</sup> L.N. Mulay and W.J. Danley, *J. Appl. Phys.* **41**, 877 (1970).
  - <sup>14</sup> L.K. Keys and L.N. Mulay, *Japan. J. Appl. Phys.* **6**, 122 (1966).
  - <sup>15</sup> W.J. Danley and L.N. Mulay, *Mat. Res. Bull.* **7**, 739 (1972).
  - <sup>16</sup> V. Eyert, U. Schwingenschlögl and U. Eckern, *Chem. Phys. Lett.* **390**, 151 (2004).
  - <sup>17</sup> I. Leonov, A.N. Yaresko, V.N. Antonov, U. Schwingenschlögl, V. Eyert and V.I. Anisimov, *J. Phys.: Condens. Matter* **18**, 10955 (2006).
  - <sup>18</sup> L. Liborio and G. Mallia, *Phys. Rev. B* **79**, 245133 (2009).
  - <sup>19</sup> M. Weissmann and R. Weht, *Phys. Rev. B* **84**, 144419 (2011).
  - <sup>20</sup> A.C.M. Padilha, J.M. Ozorio-Guillén, A.R. Rocha and G.M. Dalpian, *arXiv.org*.
  - <sup>21</sup> M. Canillas, E. Chinarro, M. Carballo-Vila, J.R. Juradoa and B. Moreno, *J. Mater. Chem. B*, **1**, 6459 (2013).
  - <sup>22</sup> G. Kresse and J. Furthmüller, *Comput. Mat. Sci.*, **6**, 15 (1996).
  - <sup>23</sup> G. Kresse and J. Furthmüller, *Phys. Rev. B*, **54**, 11169 (1996).
  - <sup>24</sup> P.E. Blochl, *Phys. Rev. B*, **50**, 17953 (1994).
  - <sup>25</sup> G. Kresse and D. Joubert, *Phys. Rev. B*, **59**, 1758 (1999).
  - <sup>26</sup> J.P. Perdew, K. Burke and M. Ernzerhof, *Phys. Rev. Lett.*, **77**, 3865 (1996).
  - <sup>27</sup> J.P. Perdew, K. Burke and M. Ernzerhof, *Phys. Rev. Lett.*, **78**, 1396 (1997).
  - <sup>28</sup> S.L. Dudarev, G.A. Botton, S.Y. Savrasov, C.J. Humphreys and A.P. Sutton, *Phys. Rev. B*, **57**, 1505 (1998).
  - <sup>29</sup> L.A. Bursil, B.G. Hyde, O. Terasaki and D. Watanabe, *Phil. Mag.* **20**, 347 (1969).
  - <sup>30</sup> A. Janotti, J.B. Varley, P. Rinke, N. Umezawa, G. Kresse and C.G. Van de Walle, *Phys. Rev. B* **81**, 085212 (2010).
  - <sup>31</sup> D. Kaplan, C. Schlenker and J.J. Since, *Philos. Mag.* **36**, 1275 (1977).
  - <sup>32</sup> M. Marezio, P.D. Dernier, D.B. McWhan and S. Kachi, *J. Solid State Chem* **11**, 301 (1974).
  - <sup>33</sup> A.S. Botana, V. Pardo, D. Baldomir, A.V. Ushakov and D.I. Khomskii, *Phys. Rev. B* **84**, 115138 (2011).
  - <sup>34</sup> M. Obara, A. Sekiyama, S. Imada, J. Yamaguchi, T. Miyamachi, T. Balashov, W. Wulfhekel, M. Yabashi, K. Tamasaku, A. Higashiya, T. Ishikawa, K. Fujiwara, H. Takagi and S. Suga, *Phys. Rev. B* **81**, 113107 (2010).
  - <sup>35</sup> R. James and C.R.A. Catlow, *Journal de Physique* **38**, 7 (1977).
  - <sup>36</sup> D. Adler, *Rev. Mod. Phys.* **40**, 714 (1968).